Incremental binding free energies of aluminum (III) vs. magnesium (II) complexes

5 AUTHORS, INCLUDING:

Jose M Mercero

Universidad del País Vasco / Euskal Herriko…

70 PUBLICATIONS   1,116 CITATIONS

SEE PROFILE

Jon I Mujika

Universidad del País Vasco / Euskal Herriko…

31 PUBLICATIONS   389 CITATIONS

SEE PROFILE

Jon M Matxain

Universidad del País Vasco / Euskal Herriko…

83 PUBLICATIONS   1,421 CITATIONS

SEE PROFILE

Xabier Lopez

Universidad del País Vasco / Euskal Herriko…

133 PUBLICATIONS   2,375 CITATIONS

SEE PROFILE

ELSEVIER

Incremental binding free energies of aluminum (III) vs. magnesium (II) complexes

Jose M. Mercero *, Jon I. Mujika, Jon M. Matxain, Xabier Lopez, Jesus M. Ugalde

Kimika Fakultatea, Euskal Herriko Unibertsitatea, PK 1072, Donostia San Sebastian, 20080 Euskadi, Spain

Abstract

A sequential ligand addition to the aluminum (III) cation has been studied using the B3LYP functional and a combined all-electron/pseudopotentials basis set. The aluminum complexes are compared with analogous magnesium (II) complexes. Different thermodynamical data, such as incremental binding energies, enthalpies, entropies and free energies, are presented for these addition reactions. While the magnesium (II) cation can only accommodate three negatively charged ligands, aluminum (III) accommodates four even after including bulk solvent effects. The main differences between both cations complexing with the neutral ligands, is that aluminum (III) is not able to form complexes with methanol until the number of methanol ligands is equal to 3. Magnesium (II) prefers to bind methanol and formamide when the number of ligands is small, while aluminum prefers formamide. For the largest complexes both cations prefer to bind water.
© 2003 Elsevier B.V. All rights reserved.

Keywords: Aluminum; Magnesium; Bio-ligands; Formate; Thiolate; Thiol; Formamide; Acetate; Methanol; Water; Metal-ligand interactions; Acetate

1. Introduction

Numerous toxic effects have been attributed to the aluminum (III) cation over the last few years. As a consequence, it has gained interest in the scientific world [1]. Aluminum (III) toxicity is based on competition with other metal cations, interfering the biological processes. It is seen to enter and permanently occupy binding sites which in healthy systems are served by other metal cations with specific binding and charge properties [2]. Magnesium (II) seems to be the most affected cation, since the two cations are similar in size, which is a dominant factor over the charge identity in terms of metal ion competition [3,4].

Similarly, interest for the mechanism of metal cation complexation has grown in the recent years. One key aspect of this interest resides in the quest for a better understanding of the metal–ligand interactions in different chemical, photochemical and biochemical processes [5–9]. Although theory has made quite a progress in the field [10], relevant to this issue are recent advances in gas-phase methods (Electrospray Ionization, Charge Striping Spectroscopy, Double-Charge Spectroscopy, Blackbody Infrared Radiative Dissociation, etc.) for they provide the opportunity to study not only mono-charged but multiple charged cations [11–15].

Recently, Dudev et al. [9] have studied the incremental binding free energies in magnesium (II) complexes [8] and compared the competitive binding between magnesium and different ligands. They observed that magnesium (II) cation cannot bind more than three formate ligands, and that among the neutral ligands magnesium (II) cation prefers to bind methanol and formamide when the number of ligands is less than four, but it prefers to bind water when the number of ligands is larger.

In previous studies of our group we compared the binding energies between the aluminum (III) and magnesium (II) cations with different ligands, the aminoacid sidechains, e.g., $YHCOO^-$, YNH_2CHO, YS^-, YSH_2, etc. (where Y stands for the different number of CH_3

---

* Corresponding author. Tel.: +34943015341; fax: +34943212236.
  E-mail address: pobmelat@sq.ehu.es (J.M. Mercero).

group until completing the aminoacid chain) [16–19]. We observed that the strongest binding energies occurred with the negatively charged ligands, i.e., the formate (YHCOO⁻) and the thiolates (YS⁻).

In this study we compare the incremental binding free energies between aluminum (III) and magnesium (II) cations and some relevant bioligands. These ligands are those modeling the sidechains of the aminoacids, and the water molecule. The formate ($HCOO^-$), is the smallest functional group representing the acidic aminoacids glutamic and aspartic acids sidechains. The anionic form has been chosen since a proton is lost at physiological pH. Formamide ($HCONH_2$), models asparagine and glutamine, methanol (CH_3OH), serine, threonine and tyrosine aminoacids, and finally, the sulfur containing cysteine aminoacid is modeled with the methyl–thiol. Note that the anionic form of the methyl–thiol (methyl–thiolate, CH_3S^-) ligand is also studied since this both forms of the aminoacids are found on a living organisms.

2. Methods

All calculations were carried out with the GAUSSIAN 98 [20] package. It has already been proven that the density functional methods give excellent results in most chemical systems [21]. DFT/HF hybrid methods are particularly appealing for the present investigation. The Becke proposed hybrid [22] (B3), together with the LYP [23] correlation functionals have been chosen for this work.

The standard all electron 6-31+G(d,p) basis set was used for the metal cations, similarly, the 6-31++G** basis was used for the hydrogen atoms. The relativistic compact effective core potentials and shared-exponent basis set of Stevens, Krauss, Barsch and Jasien (SBKJ) [24] including a polarization and a diffuse function were used for the atoms of the ligands. This pseudopotential/all-electron basis set combination for the ligand and the metal cation, respectively, was found by Gresh et al. [25–27] to represent a very well balanced compromise between accuracy and computational efficiency.

Frequencies (in order to confirm that all the structures are a minimum in the potential energy surface), thermal corrections (E_{TRV}) and entropies were calculated at this level of theory and the corresponding zero-point vibrational energy (ZPVE) corrections made to the total energy, using standard statistical mechanical methods [28]. Note that no empirical correction was applied to the frequencies. The enthalpy, and free energy changes of the complexation $M + nL \rightarrow M(L)_n$, were evaluated at 298 K as follows:

$$\Delta H = \Delta E_{elec} + \Delta E_{TRV} + \Delta ZPVE + n\Delta PV, \qquad (1)$$

$$\Delta G = \Delta H - T\Delta S_{TRV}. \qquad (2)$$

The properties described below such as the incremental enthalpies ($\Delta\Delta H$), entropies ($\Delta\Delta S$), and free energy ($\Delta\Delta G$) are evaluated in the following way:

$$\Delta\Delta X^{n-1,n} = \Delta X^n - \Delta X^{n-1}, \qquad (3)$$

where n is the number of ligands and X stands for H, S or G. This incremental magnitude is equivalent to the ΔX of:

$$ML_{n-1} + L \rightarrow ML_n. \qquad (4)$$

The natural bond-orbital theory [29–31] was used to compute charges on the atoms of these complexes.

The Molden [32] program was used to visualize and draw the figures.

3. Results

3.1. $X(H_2O)_n^{3/2}$ complexes, calibration

Few theoretical data have been published in the literature concerning aluminum trication and biologically relevant ligands. Thus, in order to calibrate our results we have focused on the hydration of the aluminum (III) cation for which experimental and previous theoretical data are available [33–36]. At the same time, we have also compared the results obtained for magnesium (II) with the data available in the literature. The incremental binding energies, enthalpies, entropies and free energies are shown in Table 1.

Several studies using different levels of theory have been performed concerning aluminum (III) cation hydration [33–35]. The $X(H_2O)_6^{3/2}$ structure is shown in Fig. 1 (3). The rest of the $X(H_2O)_n^{3/2}$ structures ($n = 1, \ldots, 5$) are given as supplementary material. Tunega et al. [34], compared different DFT functionals and MP2 combining them with different basis sets. Finally they chose the BLYP/SVP+sp level of theory. They obtained bond lengths of 1.961 and 0.991 Å for Al–O and O–H, respectively, with an H–O–H angle of 106.1°. Wasserman et al. [35] predicted 1.907 Å, 0.973 Å and 106.5° for the same properties at the MP2/cc-pVTZ level of theory. The X-ray gives an Al–O bond length of 1.87–1.90 Å (see [36] and references therein). Our geometrical values are 1.942 Å, 0.979 Å, and 107.23°, respectively, being in a very good agreement with the values, either theoretical or experimental, found on the literature. The formation energies for the $Al(H_2O)_6^{+3}$ complexes estimated by Tunega et al. [34] and Wasserman et al. [35] are −710.6 and −698.7 kcal/mol, respectively, while our calculations give a formation energy of −692.73 kcal/mol, which agrees well with these values.

The geometries and energies for the magnesium clusters also agree reasonably well with calculations and experiments reported in the literature. The X-ray diffraction method evaluates a Mg–O bond length around

Table 1
Binding energies (BE), incremental BE (ΔBE), incremental enthalpies ($\Delta\Delta H$), incremental entropy ($T\Delta\Delta S$), incremental free energies ($\Delta\Delta G$), of the given complexes, in kcal/mol

n	Symm.	BE		ΔBE		$\Delta\Delta H$		$T\Delta\Delta S$		$\Delta\Delta G$	
		Al	Mg	Al	Mg	Al	Mg	Al	Mg	Al	Mg
H_2O											
1	c2v	−203.40	−80.87	−203.40	−80.87	−203.83	−80.00	−7.30	−7.18	−205.02	−72.81
2	D2d	−370.93	−152.95	−167.53	−72.09	−165.69	−70.19	−9.45	−7.73	−156.24	−62.46
3	D3	−493.64	−208.90	−122.71	−55.94	−120.14	−53.96	−10.54	−9.63	−109.61	−44.34
4	S4	−587.42	−253.83	−93.79	−44.94	−91.35	−43.03	−9.09	−8.37	−82.26	−34.66
5	c2v	−641.67	−283.65	−54.25	−29.82	−51.54	−27.89	−11.77	−10.97	−39.76	−16.92
6	Th	−692.73	−311.07	−51.06	−27.42	−48.71	−25.75	−13.27	−12.12	−35.63	−13.63
$XHCOO^-$											
1	C2v	−710.92	−364.88	−710.92	−364.88	−709.83	−363.30	−8.84	−8.53	−700.99	−354.77
2	D2D	−1131.62	−572.91	−420.70	−208.03	−417.68	−205.63	−12.18	−10.99	−405.50	−194.64
3	D3	−1323.71	−627.81	−192.09	−54.90	−189.54	−53.34	−13.85	−11.29	−175.68	−42.06
4	S4	−1373.99	−599.29	−50.28	+28.51	−49.52	+29.34	−3.28	−4.69	−45.65	+34.03
5	c1	−1352.15	−504.40	+21.83	+94.84	+23.85	+97.12	−13.19	−10.52	+37.05	+107.65
6	S6	−1265.82	−350.90	+86.33	+153.50	+88.85	+154.62	−13.12	−9.04	+101.97	+163.65
XCH_3COO^-											
1		−742.57	−375.27	−742.57	−375.27	−742.08	−373.78	−5.23	−7.81	−736.85	−365.97
2		−1160.25	−583.07	−417.67	−207.80	−413.83	−205.38	−7.18	−11.71	−406.65	−193.67
3		−1342.79	−635.12	−182.54	−52.05	−179.89	−50.63	−10.05	−12.02	−169.85	−38.61
4		−1381.18	−603.13	−38.40	+32.04	−36.89	+33.49	−6.67	−9.62	−30.21	+43.11
$XSCH_3^-$											
1	CS	−741.13	−359.66	−741.13	−359.66	−742.16	−358.83	−6.99	−6.96	−735.17	−351.87
2	C2	−1117.87	−550.24	−376.74	−190.58	−371.52	−187.80	−10.04	−8.76	−361.48	−179.04
3	C3	−1310.97	−611.90	−193.10	−61.66	−190.84	−60.08	−10.41	−9.35	−180.43	−50.73
4	S4	−1371.20	−576.75	−60.23	+35.15	−58.86	+36.13	−10.39	−10.11	−48.47	+46.52
5	C1	−1310.33		+60.87		−61.39		−12.7		+74.09	
6	S6	−1182.75		+127.58		−189.35		−9.91		+137.87	
$XSHCH_3$											
1	Cs	–	−96.03	–	−96.03	–	−95.5	–	−7.31	–	−88.18
2	C2	−469.03	−165.28	−469.03	−69.25	−468.15	−67.57	−16.37	−8.98	−451.78	−58.6
3	C3	−565.31	−209.05	−96.28	−43.77	−63.91	−43.27	−11.21	−12.94	−82.7	−30.34
4	S4	−634.46	−242.37	−69.15	−33.32	−67.18	−30.58	−11.47	−6.82	−55.7	−23.85
5	C1	−660.95	−257.71	−26.49	−15.34	−24.67	−13.92	−11	−9.56	−13.68	−4.26
6	S6	−686.15	−273.49	−25.2	−15.78	−23.45	−14.4	−14.64	−11.48	−8.8	−2.92
Al CH_3OH											
3	C3	−575.17		−575.17		−572.34		−28.32		−544.02	
4	C2	−663.64		−88.47		−85.64		−11.12		−74.52	
5	C1	−710.15		−46.51		−43.82		−12.91		−30.90	
6	S6	−752.73		−42.58		−40.36		−11.42		−28.94	
Al $HCONH_2$											
1	C1	−323.27		−323.27		−323.28		−8.54		−314.74	
2	C2H	−547.63		−224.35		−220.56		−10.39		−210.17	
3	C3	−688.46		−140.83		−137.93		−12.09		−125.84	
4	S4	−783.74		−95.28		−92.96		−11.39		−81.57	
5	C1	−829.61		−45.87		−43.91		−12.35		−31.57	
6	S6	−874.41		−44.8		−43.00		−13.75		−29.25	

n stands for the number of ligands, and symm. corresponds to the symmetry of the complex.

2.00–2.15 Å (see [36] and references therein). The Mg–O bond length reported by Dudev and Lim [8] is 2.110 Å for the hexahydrated magnesium cation, at the B3LYP/6-31+G* level of theory. Our calculations, with the level of theory described above, predict exactly the same theoretical bond length, which is in a very good agreement with the X-ray value. The values of the Mg–O bond lengths calculated by Dudev et al. for the different $Mg(H_2O)_n^{+2}$ clusters are 1.939, 1.958, 1.986, 2.012 Å for $n = 1$–4 and 2.054, 2.049 and 2.104 Å for the different Mg–O bonds of the $n = 5$ complex, while our values are 1.942, 1.956, 1.985, 2.018 and Å 2.056, 2.050 and 2.102 Å, respectively. Notice the close agreement between the two sets of data. Experimental measurements (for the 5
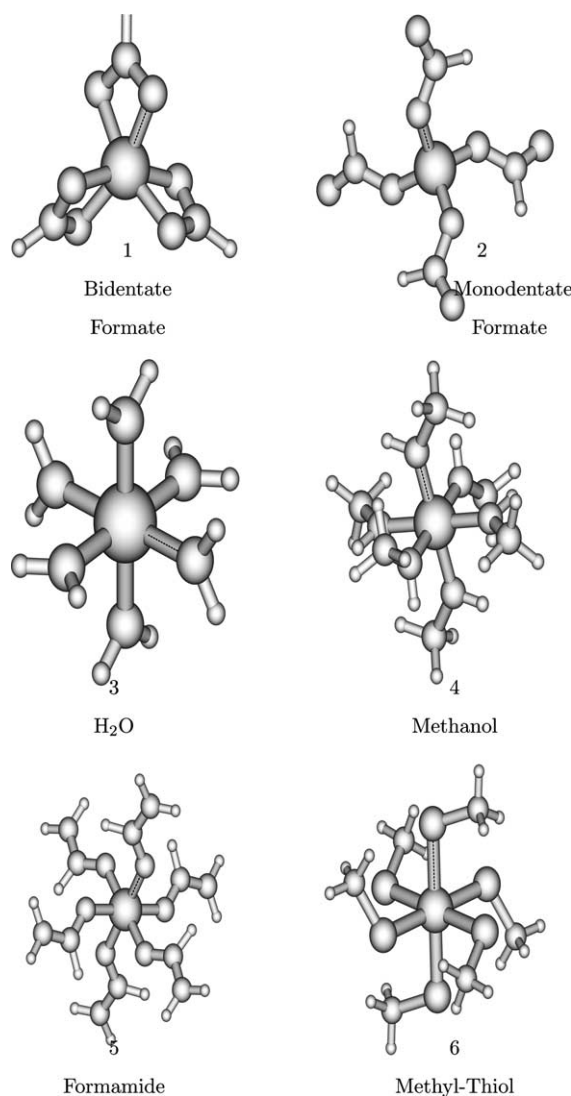
Fig. 1. 1 and 2 represent the monodentate and bidentate coordinations of the formate. 3, 4, 5 and 6 are the largest complexes for water, methanol, formamide and methyl–thiol, respectively. For the sake of brevity, only some representative structures described on the text are shown, the draws for the rest of the complexes are given as a supplementary material.

to 6 water molecules increment in the complex) using high-pressure mass spectrometry by Peschtke et al. [37] of the magnesium (II) hydration report values of -24.6 kcal/mol for the $\Delta\Delta H$ and -8.7 kcal/mol for the $T\Delta\Delta S$ while our predictions are -25.75 and -12.12 kcal/mol which agree reasonably well with the experimental values. Rodriguez-Cruz et al. [38] using electrospray ionization techniques estimate $\Delta\Delta E$ and $\Delta\Delta H$ values of -25.5 ± 1.3 and -26.3 kcal/mol for the 4 to 5 ligand increment, while our values are -29.82 and -27.89 kcal/mol, respectively. The $\Delta\Delta E$ and $\Delta\Delta H$ increase for the addition of a water molecule to the $Mg(H_2O)_5^{+2}$ complex is estimated to -23.5 ± 1.6 and -24.2 kcal/mol [38] and our predictions -27.42 and -25.75 are in a very good agreement.

With all these experimental and theoretical data available on the literature, we conclude that our level of theory using the B3LYP functional together with an all-electron (for the cation) and pseudopotentials (for the ligands) combined basis set gives very good results. The use of pseudopotentials reduces slightly the size of the calculations, reducing at the same time the CPU usage. This effect is important for the larger complexes.

3.2. Negatively charged ligands

In previous studies, we observed that aluminum (III) and magnesium (II) cations have similar binding energies with a single carboxylate ligand (-710.21 and -364.37 kcal/mol, respectively [16]) and a single thiolate ligand (-741.38 and -360.36 kcal/mol, respectively [18]). In the present work we analyze the effect of the addition of more than one ligand not only in the binding energy and geometry, but also in the enthalpy, the entropy and the free energy of the complexation reaction. In this section we study the incremental binding energies, enthalpies, entropies and free energies of the aluminum (III) and magnesium (II) cations with the negatively charged $HCOO^-$ and CH_3S^- ligands. Again, we validate our level of theory comparing the results of the $Mg–(HCOO)_n^{2-n}$ complexes with the results obtained by Dudev and Lim [8]. We extend the calculations to the $Mg–(SCH_3)_n^{2-n}$ series of complexes and compare the analogous aluminum and magnesium complexes.

The most representative structures of these complexes are shown in Fig. 1. Structures 1 and 2 show the different coordination orientations of formate and 6 shows the $Al–(SCH_3)_6^{-3}$ complex. Given these structures and the symmetries of the clusters (in Table 1) the reader can get an idea of the rest of complexes. We provide all the structures as supplementary material. Note that for the magnesium (II) cation we were not able to find any complex with more than four SCH_3^- ligands.

As it can be observed in Fig. 2, the X–O bond length for the $X–(HCOO)_n^{3/2-n}$ complexes increases going from $n = 1$ to $n = 3$, and decreases for $n = 4$, increasing again for $n = 5$ and 6 as it can be observed in Fig. 2. The same trend is due to the coordination change of the ligand, since the carboxylate interacts in a bidentate mode for $n \leqslant 3$, and in monodentate for $n \geqslant 4$ (see Fig. 2). This trend is observed for the Al–O and Mg–O bond lengths, with shorter bond lengths in the aluminum complexes (see Fig. 2). Dudev et al. reported bond lengths of 1.963, 2.040, 2.162 and 1.983 Å for the Mg–O bonds of the first four complexes, calculated at the B3LYP/6-31+G* level of theory. Our values values are 1.963, 2.037, 2.156 and 1.980 Å, respectively, which are in a very good agreement.

For the $X–(SCH_3)_n^{3/2-n}$ a smooth increase in the bond length is observed after the addition of each SCH_3^- ligand. Note that the Al–S bond length when $n = 1$ is out
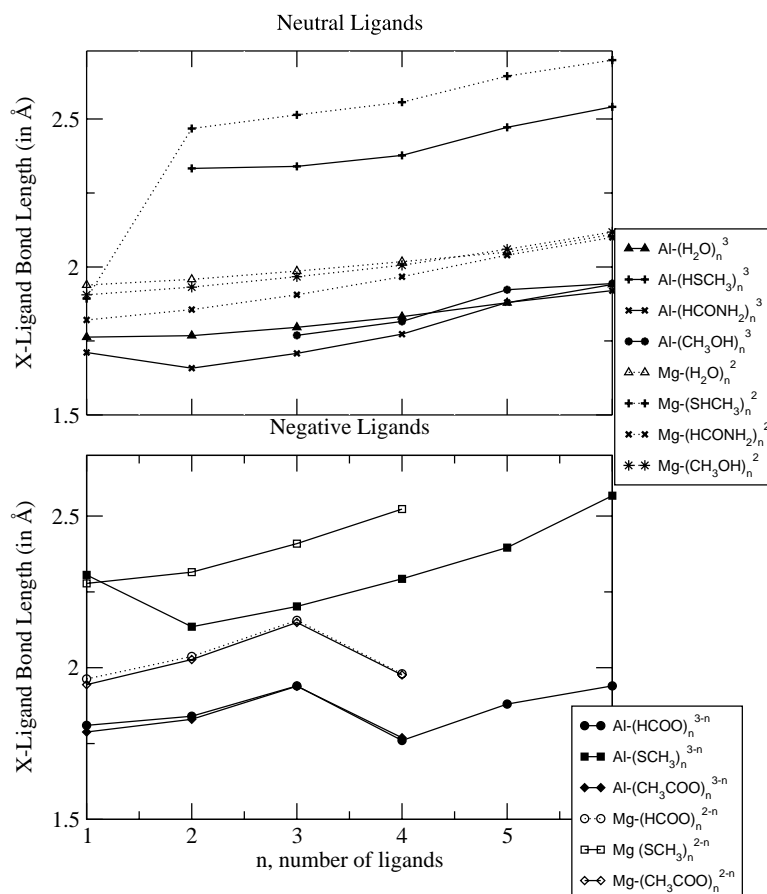
Neutral Ligands

Fig. 2. Bond lengths between the metal cation and the ligands at the discussed complexes. Mg–Formamide and Mg–Methanol bond lengths are taken from [8].

of this trend, and this bond is larger than the analogous Mg–S. Despite this point, on the whole, the Al–S bond lengths are around 0.2 Å shorter than the Mg–S bond lengths (see Fig. 2).

The binding energies, incremental binding energies, enthalpies, entropies and free energies for these complexes are shown in Table 1. A smooth decrease of the incremental binding energy (ΔBE), enthalpy ($\Delta\Delta H$) and free energy ($\Delta\Delta G$) is observed as we increase the number of ligands. $\Delta\Delta G$ is plotted in Fig. 3 for the negative ligand clusters. The changes in $\Delta\Delta G$ with the number of ligands is very similar for both aluminum (II) and magnesium (II) cations. A difference between aluminum (III) and magnesium (II) complexes is that while for magnesium the addition of a fourth ligand is thermodynamically unfavorable ($\Delta\Delta G = 34.03$ and 46.5 kcal/mol for $HCOO^-$ and SCH_3^- ligands, respectively), aluminum can accommodate a fourth ligand ($\Delta\Delta G = -45.65$ and -48.47 kcal/mol for $HCOO^-$ and SCH_3^- ligands, respectively). Addition of a fifth ligand becomes thermodynamically unfavorable for aluminum (see Table 1 for more details).

In general, the free energy gain after the addition of a new ligand is dominated by the enthalpy gain, with small contributions of the entropy gain. However, notice that increasing the number of ligands the entropic gain becomes more important in the final free energy gain. In the $Mg–(HCOO)_n^{2-n}$ clusters, when $n = 3$, the entropic gain is a fifth of the enthalpic gain, and something similar is observed for the entropy/enthalpy gain at the $Al–(SCH_3)_4^-$ complex. We have plotted the incremental entropy of these complexes (Fig. 3) and we observe a minimum corresponding to $n = 4$ for $X–(HCOO)_4^{-1/-2}$ complexes. This value is due to the change in coordination of the ligand (bidentate for $n = 3$, and monodentate for $n = 4$).

We have also analyzed the charge transfer from the ligand to the metal cation. The natural charges of the metal for the different complexes are plotted in Fig. 4. The largest charge transfer for the carboxylate complex, occurs in the $n = 3$ complexes. The natural charge of the metal cation decreases until $n = 3$, where a minimum is observed, and it increases for $n = 4$ after the type of the ligand coordination changes. The trends for aluminum and magnesium natural charges are very similar, with a larger charge transfer for the aluminum complexes (see Fig. 4). For the thiolate complexes, however, there is a different behavior of the charge transfer depending on
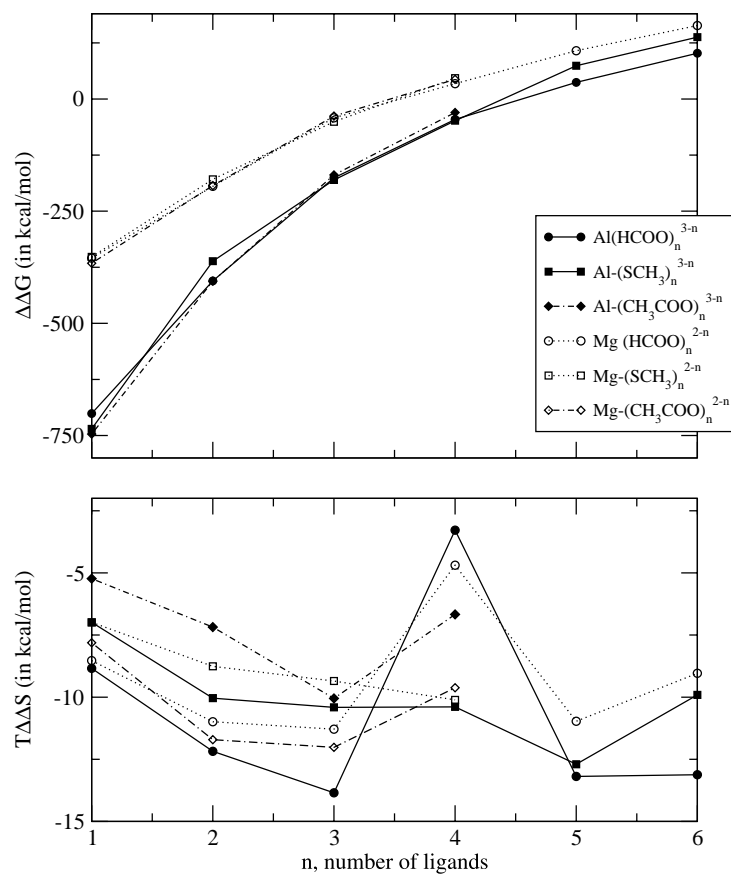
Fig. 3. Incremental free energies , $\Delta\Delta G$, and incremental entropy (on the bottom), $T\Delta\Delta S$ (in kcal/mol) of the negative ligand clusters as a function of the number of ligands.
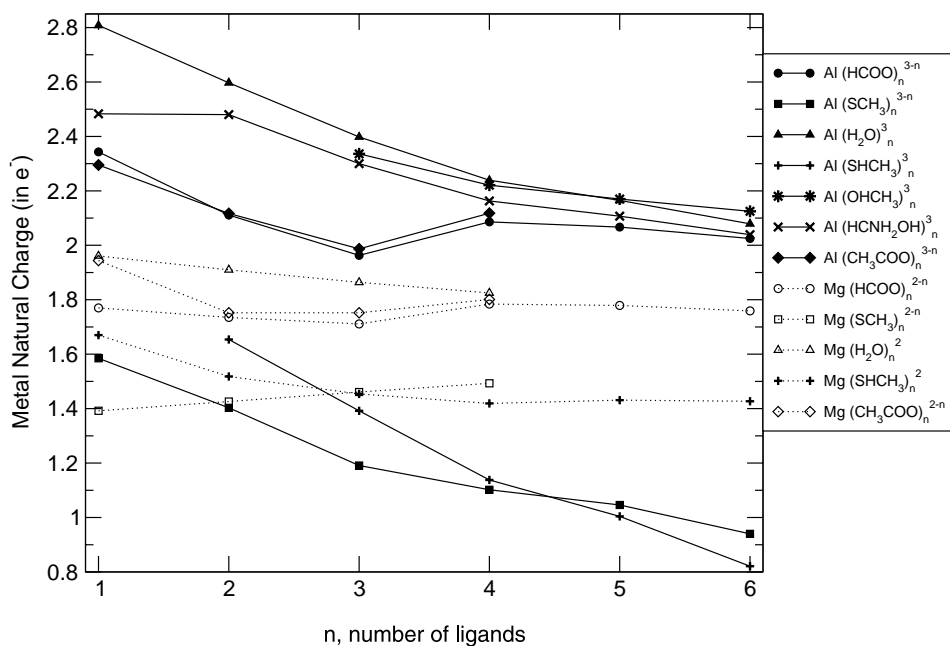

Fig. 4. Natural charge (in e$^-$) of the metal cations as a function of the number of ligands.

the metal cation. The charge transfer for the aluminum is larger as n increases, for magnesium, however, the opposite effect is observed, the charge transfer decreases as n increases.

Comparing the $HCOO^-$ and the SCH_3^- ligands, we observe that aluminum prefers binding to the SCH_3^- ligand when $n = 1$, while magnesium has larger affinity for the formate, the binding energy is only 5 kcal/mol larger than the thiolate's one. Garmer and Gresh [25] back in 1994, studied similar magnesium complexes and reported formate to be favored in 13 kcal/mol, (optimizing the complexes at the HF level of theory with SBKJ pseudopotentials for the ligand and 6-631G for magnesium, and refining the energies by the MP2 expansion). They rationalized this binding energy difference between these complexes by the Reduced Variational Space [39] (RVS) energy decomposition scheme. They data showed that the preference of the formate is mainly due to the electronic energy term, since contributions of the charge transfer and polarization were slightly larger in the $Mg–(SCH_3)^{+1}$ complex (see [25] for more details). These two energy contributions could be the key aspects to elucidate the different binding preference of the aluminum cation. The +3 charge of the aluminum will lead to a larger polarization of the thiol than the formate, and similarly, the charge transfer will also be larger (as it is shown in Fig. 4). The energy contribution of these properties will be larger than that of in the formate, leading to a larger binding energy between the aluminum and the thiol.

We have previously observed that the addition of methyl groups increases the interaction energy of the ligand either with aluminum or magnesium [16,18]. The addition of the methyl group into the formate, increases its polarizability, and also the charge transfer from the ligand to the metal cation, leading to a larger contribution of the energetic terms associated to these properties. Thus, we have also calculated the $X–(CH_3COO)_n^{3/2-n}$ complexes, which also have a methyl group, and are closer in size to the $X–(SCH_3)_n^{3/2-n}$ complexes. The addition of the methyl group to the formate increases the binding free energy being now very similar to that of the $Al(SCH_3)_1^{+2}$ complex. Irrespective of the size of the complex the free energy increase converges to similar values for the three different ligands from $n = 1$ to $n = 4$. Then the smaller the ligand the larger the free energy gain, due to smaller steric effects.

3.3. Neutral ligands

In this section we study the incremental binding energies, enthalpies, entropies and free energies of the aluminum (III) complexes with methanol, formamide and thiol ligands. The data obtained by Dudev et al. for the magnesium (II) complexes have been used to com-

pare with the analogous aluminum (III) complexes. In order to accomplish a complete study of these biologically relevant ligands, we have also studied the interactions between the thiol and the magnesium (II) cation.

For the sake of brevity only the most representative complexes for $X–(CH_3OH)_n^{3/2}$, $X–(HCONH_2)_n^{3/2}$ and $X–(HSCH_3)_n^{3/2}$ are shown in Fig. 1. Based on the pictures therein and the symmetries of the complexes shown in Table 1, one can get a picture of the rest of the complexes, which are given as supplementary material. No $Al–(CH_3OH)_n^{3/2}$ complexes were found for $n < 3$. All the attempts to locate $Al–(CH_3OH)_{1/2}^{+3}$ lead to similar structures. For $n = 2$ complexes, a charge transfer occurring from the methyl group into the $Al(OH)_2^{+1}$ complex, was observed, following a dissociation into an $Al(OH)_2^{+1}$ complex, and two CH_3^+ cations. For the $n = 1$ complex, similarly, dissociation into $Al(OH)^{+2}$ and a CH_3^+ was obtained. We did not find either any $Al–(SHCH_3)_1$ complex as we described and studied in detail in [18]. In this case, the minimization leads to $AlSH^{+2}$ and CH_3^+.

On the whole, as for the negative ligand containing complexes, the X–L bond length increases with the number of ligands (see Fig. 2). The shortest bonds are between the Al and the formamide ligand, while the Al–methanol bond lengths are slightly longer. On the contrary, the complexes formed with the $SHCH_3$ ligand present the largest X–L bond length due to the size of the sulfur atom. The Mg–S bonds are also the largest of the magnesium complexes. Beside the X–S bond lengths, the rest of the X–L bond lengths start being different for $n = 1$ and they tend to similar bond lengths for $n = 6$. These complexes show similar trends for the ΔBE, $\Delta\Delta H$ and $\Delta\Delta G$ as it is shown in Table 1. For the smallest complexes, as for the negative ligand containing complexes, the contribution of the entropy gain on the free energy gain is small comparing to the contribution of the enthalpy gain. However, for the largest complexes the entropic contributions become more important. When $n > 4$, the $T\Delta\Delta S$ is nearly half of the $\Delta\Delta H$ in the aluminum thiol complexes, and a fourth in the others. For the magnesium complexes, as reported by Dudev et al., the entropic contribution is almost the half of the enthalpy gain in the largest complexes. It is interesting to note that while the enthalpy gain in the aluminum complexes is significantly larger than in the magnesium ones, the entropy gain is very similar (see Fig. 5).

Comparing the $Mg(SHCH_3)_n^{2+}$ complexes with the previously calculated MgL (L = H_2O, CH_3OH and $HCONH_2$) complexes by T. Dudev and Lim [8], the $\Delta\Delta G$ when $n = 1$ is similar to the $Mg(CH_3OH)_1^{+2}$. However, the $\Delta\Delta G$ for the $Mg(SHCH_3)_n^{2+}$ decreases more rapidly as n increases.

The charge of the metal cations is plotted in Fig. 4. As found for the negative ligands, the largest charge transfer occurs with the sulfur containing ligand, i.e., the
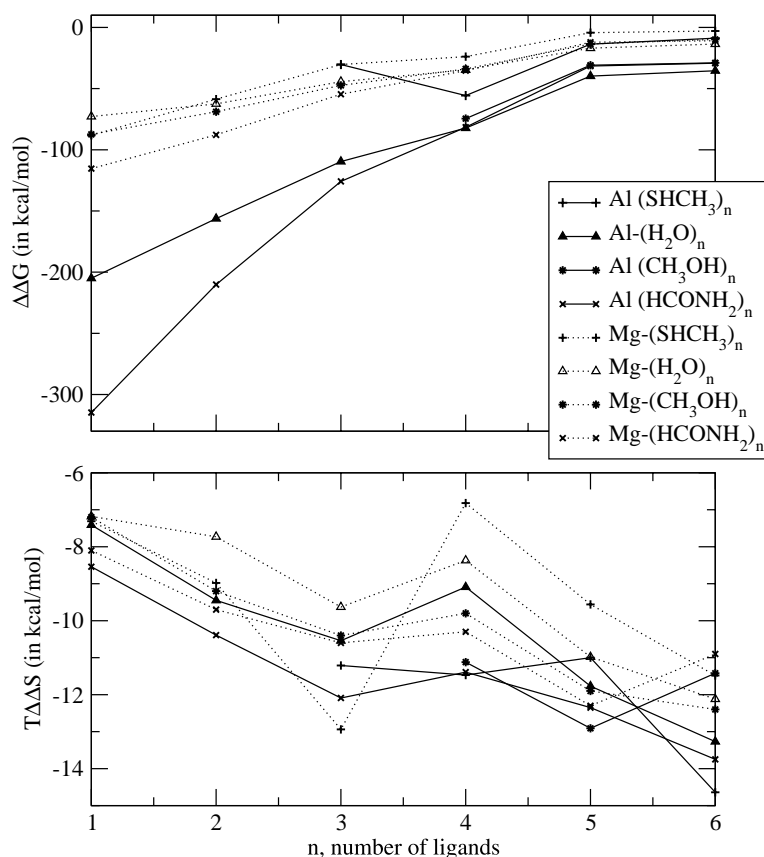
Fig. 5. Incremental free energies, $\Delta\Delta G$, and incremental entropy (on the bottom), $T\Delta\Delta S$ (in kcal/mol) of the neutral ligand clusters as a function of the number of ligands.

thiol. The charge transfer is smaller for the H_2O, CH_3OH and $HCONH_2$ ligands and it increases with the size of the complexes. The largest charge transfer occurs for the Al–$(HSCH_3)_6^{+3}$ cluster for which aluminum shows a natural charge of 0.8 e$^-$.

The preferential binding of both metals is very similar, with the exceptions of methanol, where we only found aluminum–methanol complexes for $n > 2$ and thiol, where no Al–$(CH_3SH)_1^3$ complex was found (see [18]). Dudev et al. observed that magnesium (II) cation prefers to bind formamide and methanol for $n > 4$, in our data thiol is located close to the methanol in the binding preference ranking. For the largest clusters, however, the magnesium prefers binding to water, methanol, formamide and thiol, respectively. The aluminum (III) cation presents a similar trend. It only binds formamide and water for $n = 1$, preferring formamide over water. For $n = 4$, when we are able to optimize structures with any of the ligands, aluminum (III) preference ranking is water, formamide, methanol, which have similar $\Delta\Delta G$, and thiol. The same order is maintained for $n = 6$, the $\Delta\Delta G$ being now nearly degenerate for the formamide and methanol complexes.

4. Discussion

The clustering of these compounds is governed mainly by two factors: the charge transfer suffered by the metal, and the steric effects after the increasing of the solvation shell. Upon the addition of the first ligand the positive charge of the metal cation decreases as a consequence of the charge transfer from the ligand to the metal. Hence, the incoming second ligand finds a less positively charged cation to interact (electrostatically) with and, consequently, the electrostatic interaction energy of the second ligand is smaller than that of the first ligand. Addition of other ligands should follow this trend of diminishing the electrostatic interaction energy. On the other hand, steric repulsion energies should grow larger as the first coordination shell gets more crowded with the increasing number of ligands. Due to these two effects, the X–L bond lengths increases as we increase the size of the complex, as can be seen in both graphs of Fig. 2. However, we have observed that the Mg–$(SCH_3)_n^{2-n}$ clusters follow a contradictory trend in terms of charge transfer, since the charge of the magnesium cation is more positive as the size of the ligand increases. A third factor should also be considered for the

negatively charged ligands: the coulomb repulsion energy between an anionic ligand and a negatively charged ML_n^{-1} complex. When we try to add an anionic ligand to AlL_4^- or MgL_3^-, there is a electronic repulsion between the two anions, which makes the addition of another ligand to the anionic complex unfavorable, i.e., $\Delta\Delta G > 0$. When the charge of the complex is −1, and we intent to add another negative ligand, the charge repulsion is very important. Observe that the addition of the fourth (for magnesium) and fifth (for aluminum) ligand, is unfavorable.

The change in enthalpy and free energy after the addition of the ligands may also be explained in terms of the previous factors. For the anionic ligand clusters, the gain in free energy is similar for the $HCOO^-$ and CH_3COO^- in the smallest clusters. When the number of ligands is larger than five, the $\Delta\Delta G$ of the smallest ligand complex is larger due to the smaller steric effects.

Within the neutral ligand complexes, the largest free energy gain for the aluminum (III) occurs for the formamide ligand, until $n = 4$, then, for complexes with $n > 4$ the water ligand addition is the one having a larger $\Delta\Delta G$. This is similar to the magnesium (II) behavior as reported in [8]. The only difference between the aluminum (III) and magnesium (II) is that no Al–$(SHCH_3)_1^{+3}$ nor Al–$(CH_3OH)_{1-2}^{+3}$ were found. On the contrary, for both metals, the CH_3SH ligand is the one that has the smallest free energy gain of the series after the sequential addition of ligands either for the aluminum (III) and magnesium (II). These observations could easily be understood in terms of the properties described above, i.e., the steric effects and the charge transfer. The methanol and formamide are better electron donors than water, but on the contrary, water is the smallest ligand. Thus, when the size of the complex increases and the steric effects become more important, the free energy gain of the water complex is larger.

Finally, we have investigated whether bulk solvent effects would stabilize the dianionic complexes when fully solvated, so that the resultant $\Delta\Delta G$ would be negative. The bulk solvent effects were evaluated with the PCM [40–42] model, at the HF/6-31+G* level of theory, over the gas-phase geometries obtained at the level of theory described in Section 2. We found that $(Al/Mg)L_{5/4}^{-2}$ complexes are stabilized by the bulk solvent, however, this stabilization is not big enough to make $\Delta\Delta G$ negative. Namely, the $\Delta\Delta G$ for the dianionic carboxylate complexes is reduced to 19.17 and 11.90 kcal/mol for aluminum and magnesium, respectively, while the stabilization of the dianionic thiolate complexes leads to $\Delta\Delta G$'s of 35.94 and 16.85 kcal/mol for aluminum and magnesium, respectively. In summary, it is not expected that bulk solvent would stabilize dianionic complexes so as to lead to favorable negative formation free energies.

5. Conclusions

In this study we have observed that while magnesium can only accommodate three negatively charged ligands, aluminum is capable to accommodate four, either formate or thiolate ligands. For neutral ligands, the behavior of both cations is very similar. The main difference is the lack of aluminum (III)–methanol and –thiol complexes for $n < 3$ and $n = 1$, respectively. The binding to formamide and methanol is more favorable for both cations for the smallest clusters. However, when the number of ligands increases, for both cations water is favored over the rest of the ligands.

The clustering of these compounds is mainly governed by two factors: the charge transfer suffered by the metal, and the steric effects after the increasing of the solvation shell. The charge transfer is more important in the small clusters. The steric effects, however, become very important as the size of the complex increases, e.g., water, which is the smallest ligand, it is the one preferred by the metal cations for the largest clusters ($n = 5$ and 6). In the case of anionic ligands, when the number of ligands added is so as to lead to an anionic XL_n complex, one has to take into account the coulomb repulsion between this anionic complexes and an additional negatively charged ligand, to explain the trends in $\Delta\Delta G$ for adding more ligands to the cluster.

The effect of the solvent has also been studied in order to check if dianionic complexes would be formed in a polar media. These complexes are stabilized substantially, however, the net stabilization is not large enough as to make their formation favorable.

References

[1] R.J.P. Williams, Coor. Chem. Rev. 149 (1996) 1.
[2] T.L. Macdonald, R.B. Martin, Trends Biochem. Sci. 13 (1988) 15.
[3] R.B. Martin, Clin. Chem. 32 (1986) 1797.
[4] P.O. Ganrot, Environ. Health Perspect. 65 (1986) 363.
[5] A.F. Williams, C. Floriani, A.E. Merbach (Eds.), Perspectives in Coordination Chemistry, VCHA, Basel, 1992.
[6] J. Burgess, Ions in Solution: Basic Principles of Chemical Interactions, Ellis Horwood Ltd., Chichester, UK, 1988.
[7] D.T. Richens, The Chemistry of Aqua Ions, Wiley, Chichester, England, 1997.
[8] T. Dudev, C. Lim, J. Phys. Chem. A 103 (1999) 8093.
[9] T. Dudev, J.A. Cowan, C. Lim, J. Am. Chem. Soc. 121 (1999) 7665.

[10] N. Russo, D.R. Salahub (Eds.), Metal–Ligand Interactions in Chemistry, Physics and Biology, Nato Science Series. Series C: Mathematical and Physical Sciences, vol. 546, Kluwer Academic Publishers, Dordrecht (The Netherlands), 2000.

[11] D. Schröder, H.J. Schwarz, J. Phys. Chem. A 103 (1999) 7385.

[12] M.H. Allen, T.W. Hutchens, Rapid Commun. Mass Spectrom. 308 (1992) 6.

[13] T.W. Hutchens, M.H. Allen, Rapid Commun. Mass Spectrom. 469 (1992) 6.

[14] S.E. Rodriguez-Cruz, A. Jockusch, E.R. Williams, J. Am. Chem. Soc. 120 (1998) 5842.

[15] S.E. Rodriguez-Cruz, A. Jockusch, E.R. Williams, J. Am. Chem. Soc. 121 (1999) 1986.

[16] J.M. Mercero, J.E. Fowler, J.M. Ugalde, J. Phys. Chem. A 102 (35) (1998) 7006.

[17] J.M. Mercero, J.E. Fowler, J.M. Ugalde, J. Phys. Chem. A 104 (2000) 7053.

[18] J.M. Mercero, X. Lopez, A. Irigoras, J.E. Fowler, J.M. Ugalde, J. Phys. Chem. A 105 (2001) 1986.

[19] J.M. Mercero, X. Lopez, J.M. Matxain, J.E. Fowler, J.M. Ugalde, Int. J. Quantum Chem. 90 (2002) 859.

[20] M.J. Frisch, G.W. Trucks, H.B. Schlegel, G.E. Scuseria, M.A. Robb, J.R. Cheeseman, V.G. Zakrzewski, J.A. Montgomery, R.E. Stratmann, J.C. Burant, S. Dapprich, J.M. Millam, A.D. Daniels, K.N. Kudin, M.C. Strain, O. Farkas, J. Tomasi, V. Barone, M. Cossi, R. Cammi, B. Mennucci, C. Pomelli, C. Adamo, S. Clifford, J. Ochterski, G.A. Petersson, P.Y. Ayala, Q. Cui, K. Morokuma, D.K. Malick, A.D. Rabuck, K. Raghavachari, J.B. Foresman, J. Cioslowski, J.V. Ortiz, B.B. Stefanov, G. Liu, A. Liashenko, P. Piskorz, I. Komaromi, R. Gomperts, R.L. Martin, D.J. Fox, T. Keith, M.A. Al-Laham, C.Y. Peng, A. Nanayakkara, C. Gonzalez, M. Challacombe, P.M.W. Gill, B.G. Johnson, W. Chen, M.W. Wong, J.L. Andres, M. Head-Gordon, E.S. Replogle, J.A. Pople, Gaussian 98, A11, Gaussian, Inc., Pittsburgh PA, 1998.

[21] J. Labanowski, J. Andelzelm, Density Functional Methods in Chemistry, Springer-Verlag, New York, 1991.

[22] A.D. Becke, J. Chem. Phys. 98 (1993) 5648.

[23] C. Lee, W. Yang, R.G. Parr, Phys. Rev. B. 37 (1988) 785.

[24] W.J. Stevens, M. Krauss, H. Basch, P.G. Jasien, Can. J. Chem. 70 (1992) 612.

[25] D.R. Garmer, N. Gresh, J. Am. Chem. Soc. 116 (1994) 3556.

[26] N. Gresh, W.J. Stevens, M. Krauss, J. Comp. Chem. 16 (1995) 843.

[27] N. Gresh, D.R. Garmer, J. Comp. Chem. 17 (1996) 1481.

[28] D.A. McQuarrie, Statistical Mechanics, Harper Row, New York, 1976.

[29] E.D. Glendening, A.E. Reed, J.E. Carpenter, F. Weinhold, Nbo version 3.1.

[30] J. Foster, F. Weinhold, J. Am. Chem. Soc. 102 (1980) 7211.

[31] A.E. Reed, L.A. Curtiss, F. Weinhold, Chem. Rev. 88 (1988) 899.

[32] Molden, Available from http://www.caos.kun.nl/schaft/molden/molden.html.

[33] J.D. Kubicki, D.S. amd, S.E. Apitz, J. Phys. Chem. A 103 (1999) 903.

[34] D. Tunega, G. Haberhauer, M. Gerzabek, H. Lischka, J. Phys. Chem A 104 (2000) 6824.

[35] E. Wasserman, J.R. Rustad, S.S. Xantheas, J. Chem. Phys. 106 (1996) 9769.

[36] H. Ohtaki, T. Radnai, Chem. Rev. 93 (1993) 1157.

[37] M. Peschtke, A.T. Blades, P. Kebarle, J. Phys. Chem. 102 (1998) 9978.

[38] S.E. Rodriguez-Cruz, R.A. Jockusch, E.R. Williams, J. Am. Chem. Soc. 121 (1999) 8898.

[39] W.J. Stevens, W. Fink, Chem. Phys. Lett. 139 (1987) 15.

[40] S. Miertus, E. Scrocco, J. Tomasi, Chem. Phys. 55 (1981) 117.

[41] S. Miertus, J. Tomasi, Chem. Phys. 65 (1982) 239.

[42] M. Cossi, V. Barone, R. Cammi, J. Tomasi, Chem. Phys. Lett. 255 (1996) 327.